Electronic Supplementary Material (ESI) for ChemComm.

Supporting Information for:

Dithioamide Substitutions in Proteins: Effects on thermostability, peptide binding, and fluorescence quenching in calmodulin

Christopher R. Walters,[a] John J. Ferrie,[a] and E. James Petersson[a,*]

[a]Department of Chemistry, University of Pennsylvania, 231 S. 34th Street, Philadelphia, PA, 19104, USA

*ejpetersson@sas.upenn.edu

Materials and Methods

General Information

Fmoc protected amino acids and peptide coupling reagents as well 2-chlorotrityl resin were purchased from EMD Millipore (Billerica, MA, USA). Piperidine was purchased from American Bioanalytical (Natick, MA, USA). Triisopropylsilane (TIPS) was purchased from Santa Cruz Biotechnology, Inc (Dallas, TX, USA). Isopropyl β-D-1-thiogalactopyranoside (IPTG) was purchased from LabScientific, Inc (Highlands, NJ, USA). Protease inhibitor tablets were purchased from Roche Boehringer Mannheim (Indianapolis, IN, USA). Sodium 2-mercaptoethanelsulfonate (MES•Na) was purchased from TCI America (Portland, OR, USA). FPLC purification of proteins was performed on an ÄKTA system with HiTrap Q columns (GE Healthcare Bio-Sciences, Pittsburgh, PA, USA), while peptide HPLC was performed on a Varian Prostar system (currently Agilent Technologies, Santa Clara, CA, USA) for CaM. Thiopropyl sepharose 6b resin was also purchased from GE Healthcare (Princeton, NJ, USA). Cuvettes for CD spectroscopy were purchased from Hellma Analytics USA (Plainview, NY, USA). All other reagents, solvents, and materials were purchased from either Fisher Scientific (Pittsburgh, PA, USA) or Sigma-Aldrich (St. Louis, MO, USA) unless otherwise specified. Matrix assisted laser desorption/ionization mass spectrometry (MALDI) was performed on a Bruker Ultraflex III mass spectrometer (Billerica, MA). Common abbreviations for all other chemicals are as follows: 2-(1H-benzotriazol-1-yl)-1,1,3,3-tetramethyluronium hexafluorophosphate (HBTU), *N,N*-diisopropylethylamine (DIPEA), trifluoroacetic acid (TFA), 1,2-ethanedithiol (EDT), 1,8-diazabicyclo(5.4.0)undec-7-ene (DBU), 4-(2-hydroxyethyl)-1-piperazineethanesulfonic acid (HEPES), tris(2-carboxyethyl)phosphine (TCEP), and

guanidinium hydrochloride (Gdn•HCl). Fluorescence spectra were collected on a Photon Technologies International (PTI) QuantaMaster40 fluorometer (currently Horiba Scientific, Edison, NJ, USA).

Synthesis and Characterization of CaM^{SS}

Synthesis of Thioamino Acid Precursors (Fmoc-Aa^{S}-NBt)

All thioamino acid precursors were synthesized as Fmoc-thionitrobenzotriazolide monomers (Fmoc-Aa^{S}-NBt) by starting with commercially available Fmoc protected amino acids and using a route modified from Shalaby *et al.* (See scheme **S1**).[1] Each thioamino acid precursor used in these studies has been previously synthesized and characterized.[1, 2]

Synthesis of Thioamide Containing Peptides for NCL

SPPS of monothioamide and dithioamide peptides was performed on 2-chlorotrityl resin (100-200 mesh) in 10 mL reaction vessels. The reaction scale was 50 μmol for monothioamide peptides and 100 μmol for dithioamide peptides. The resin was swelled in DMF (6 mL, 1 hour) while stirring. The vessel was then drained and to it was added the first amino acid (Fmoc-Lys(Boc)-OH; 5 equivalents) and DIPEA (10 equivalents) in DMF (4 mL). This initial loading reaction stirred for 45 minutes at room temperature (RT) before being drained, washed with DMF (2 x 4 mL) and repeated. Fmoc removal prior to thioamide couplings was performed by adding to the resin a solution of 20 % v/v piperidine in DMF (5 mL total volume) and stirring for 20 minutes at RT. The vessel was then drained and the resin washed with DMF, followed by DCM (2 x 4 mL DMF, 2 x 4 mL DCM, then 4 mL DMF). The peptide was then elongated up to the thioamide position using standard

SPPS protocols by adding 5 equivalents of amino acid and HBTU, and 10 equivalents of DIPEA in DMF (4 mL) and stirring each coupling for 45 minutes at RT. For thioamide couplings, each Fmoc-Aa^{S}-NBt (3 equivalents) precursor was added to the vessel with DIPEA (2 equivalents) in DCM (2 mL) and the reaction was stirred at RT for 30 minutes. The vessel was then drained and the resin washed with dry DCM (2 x 4 mL) before the thioamide coupling was repeated. At completion of the second coupling, the resin was washed with DCM then DMF (2 x 4 mL) and Fmoc deprotection proceeded by adding to the resin a 2 % v/v DBU in DMF solution (2 mL total volume). This DBU deprotection reaction was stirred for 2 minutes at RT. Then, the vessel was drained and the resin washed with DMF and DCM (2 x 4 mL DMF, 2 x 4 mL DCM, then 4 mL DMF). This procedure was repeated twice more before proceeding to the next amino acid coupling reaction. All subsequent Fmoc deprotections were performed using this DBU method. Standard SPPS was used to add the remaining oxo amino acids, and in the case of the dithiopeptides, the second thioamino acid coupling was done as described above. After the last Fmoc group was removed, the resin was washed with DMF, followed by DCM (2 x 4 mL each). A cleavage cocktail was prepared with 24:16:1:1:1 DCM:TFA:TIPS:EDT:Thioanisole (total volume of 4.3 mL). This was added to the resin and allowed to stir at RT for 1 hour before being drained and collected. DCM (6 mL) was added to the resin to wash out any remaining peptide and the collected solution was dried to a colorless oil (or yellow oil in the case of Tyr^{S} containing peptides) by rotary evaporation. The crude peptide product was then precipitated by adding cold diethyl ether (20 mL) and vortexing vigorously. The resulting precipitate was dried and stored under argon at -20 °C until HPLC analysis proceeded.

HPLC Purification of Thiopeptides

Monothioamide peptides were purified as previously described by Walters *et al*.[2] Dithioamide crude peptide samples were dissolved in 40 % acetonitrile in Milli-Q H_2O with 0.1 % TFA (10 mL final volume). 5 µL of a 0.5 M solution of TCEP Bond Breaker™ was added to each sample to reduce any Cys disulfides that formed during deprotection and the sample was filtered through a 0.22 µm filter. HPLC purification was performed using a Grace VyDac C18 Preparatory column (flow rate of 12 mL/min) and the gradients listed in Table **S1**. Collected fractions were analyzed by MALDI-MS for the presence of the desired dithiopeptide mass (see Table **S2**). Additionally, MALDI-TOF tandem MS/MS fragmentation experiments and corresponding analysis was performed on each of the dithiopeptides to verify that both thioamides were intact.

***Table S1*:** HPLC purification gradients for CaM dithiopeptides. Buffer A: Milli-Q H_2O with 0.1 % TFA. Buffer B: Acetonitrile with 0.1 % TFA.

Peptides	Time (min)	Buffer A (%)	Peptides	Time (min)	Buffer A (%)
H_2N-CVNYEEF^{S}V^{S}QMMTAK-OH	0	98	**H_2N-CV^{S}NY^{S}EEFVQMMTAK-OH**	0	98
H_2N-CVNY^{S}EEFV^{S}QMMTAK-OH	5:00	98		5:00	98
	10:00	75		10:00	70
	34:00	62		38:00	65
	35:00	2		39:00	2
	40:00	2		44:00	2
	41:00	98		45:00	98
	46:00	98		50:00	98
H_2N-CV^{S}NYEEFV^{S}QMMTAK-OH	0	98	**H_2N-CV^{S}NYE^{S}EFVQMMTAK-OH**	0	98
	5:00	98	**H_2N-CVNY^{S}E^{S}EFVQMMTAK-OH**	5:00	98
	10:00	70		10:00	70
	30:00	63		30:00	63
	31:00	2		32:00	2
	36:00	2		40:00	2
	37:00	98		42:00	98
	41:00	98		46:00	98

***Table S2*:** MALDI-MS observed masses for dithiopeptides and corresponding isolated yields after HPLC purification.

$CaM_{135-148}$ Sequence	Calculated m/z $[M+H]^+$	Observed m/z	% yield
H_2N-CVNYEEF^{S}V^{S}QMMTAK-OH	1724.69	1724.74	1.2
H_2N-CVNY^{S}EEFV^{S}QMMTAK-OH	1724.69	1724.92	1.2
H_2N-CV^{S}NYEEFV^{S}QMMTAK-OH	1724.69	1723.33	8.3
H_2N-CV^{S}NY^{S}EEFVQMMTAK-OH	1724.69	1725.19	2.2
H_2N-CV^{S}NYE^{S}EFVQMMTAK-OH	1724.69	1724.54	2.2
H_2N-CVNY^{S}E^{S}EFVQMMTAK-OH	1724.69	1723.49	2.5

Synthesis, Purification, and Iodoacetamide Capping of CaM^{SS}

Native chemical ligation reactions were run as described previously with no changes to protocol with respect to dithiopeptides.[2] In short, ligation buffer (500 µL, 0.2 M NaH_2PO_4, 6 M Gdn•HCl, 20 mM TCEP•HCl and 2% v/v thiophenol, pH 7.3 was added to approximately 10 mg (660 nmol) of CaM_{1-134}-MES. Thiopeptide (2 equiv) was then weighed out into a separate Eppendorf tube and ligation buffer (500 µL) was added. The thiopeptide was then added to the tube containing the CaM_{1-134}-SPh protein and incubated at 37 °C with shaking (500 RPM). After 20 hours, reactions were quenched by adding 2 mL of Milli-Q water and dialyzing twice against 2 L of 20 mM Tris pH 8.0 buffer (2 hours each) at room temperature in preparation for FPLC anion exchange chromatography using the gradient outlined in Table **S3.** It should be noted that the crude samples need to be treated with 15 µL of a 0.5 M solution of TCEP Bond Breaker™ to reduce disulfides prior to FPLC purification. Collected FPLC fractions were analyzed by MALDI-MS and fractions containing the product mass were pooled and dialyzed against 20 mM Tris, 1 mM EDTA, pH 7.5 in preparation for thiopropyl sepharose purification. Using 0.75 g of dry thiopropyl sepharose for each CaM^{SS} product, CaM^{SS} was separated

from the CaM_{1-134}-OH hydrolysis byproduct as previously described.[2] The resulting pure eluent was dialyzed against 20 mM Tris pH 8.0 buffer (2 L) for 2 hours prior to capping with iodoacetamide. Capping reactions were run as previously described[2] with the exception that fewer equivalents of iodoacetamide were used (25 mM final concentration in each sample) to potentially avoid any aberrant thioamide alkylation. Reactions were incubated with agitation for ten minutes and monitored by MALDI. At completion, the reactions were dialyzed twice against water (2 L for 2 hours each) at room temperature before being flash frozen in liquid N_2 and lyophilized to a powder.

***Table S3*:** Gradient used for anion exchange purification of CaM^{SS} NCL products. Buffer A: 20 mM Tris, pH 8.0. Buffer B: 20 mM Tris, 1 M NaCl, pH 8.0.

Time (min)	Buffer B (%)
0:00	10
10:00	10
15:00	25
70:00	40
80:00	40
80:01	100
90:00	100

***Table S4*:** Synthetic yields for CaM^{SS} proteins.

CaM Variant	Percent Yield
$Cys^{Q}_{135}Tyr^{S}_{138}Val^{S}_{142}$	5.1 %
$Cys^{Q}_{135}Phe^{S}_{141}Val^{S}_{142}$	5.9 %
$Cys^{Q}_{135}Val^{S}_{136}Val^{S}_{142}$	3.3 %
$Cys^{Q}_{135}Val^{S}_{136}Glu^{S}_{139}$	5.1 %
$Cys^{Q}_{135}Val^{S}_{136}Tyr^{S}_{138}$	2.0 %
$Cys^{Q}_{135}Tyr^{S}_{138}Glu^{S}_{139}$	1.9 %

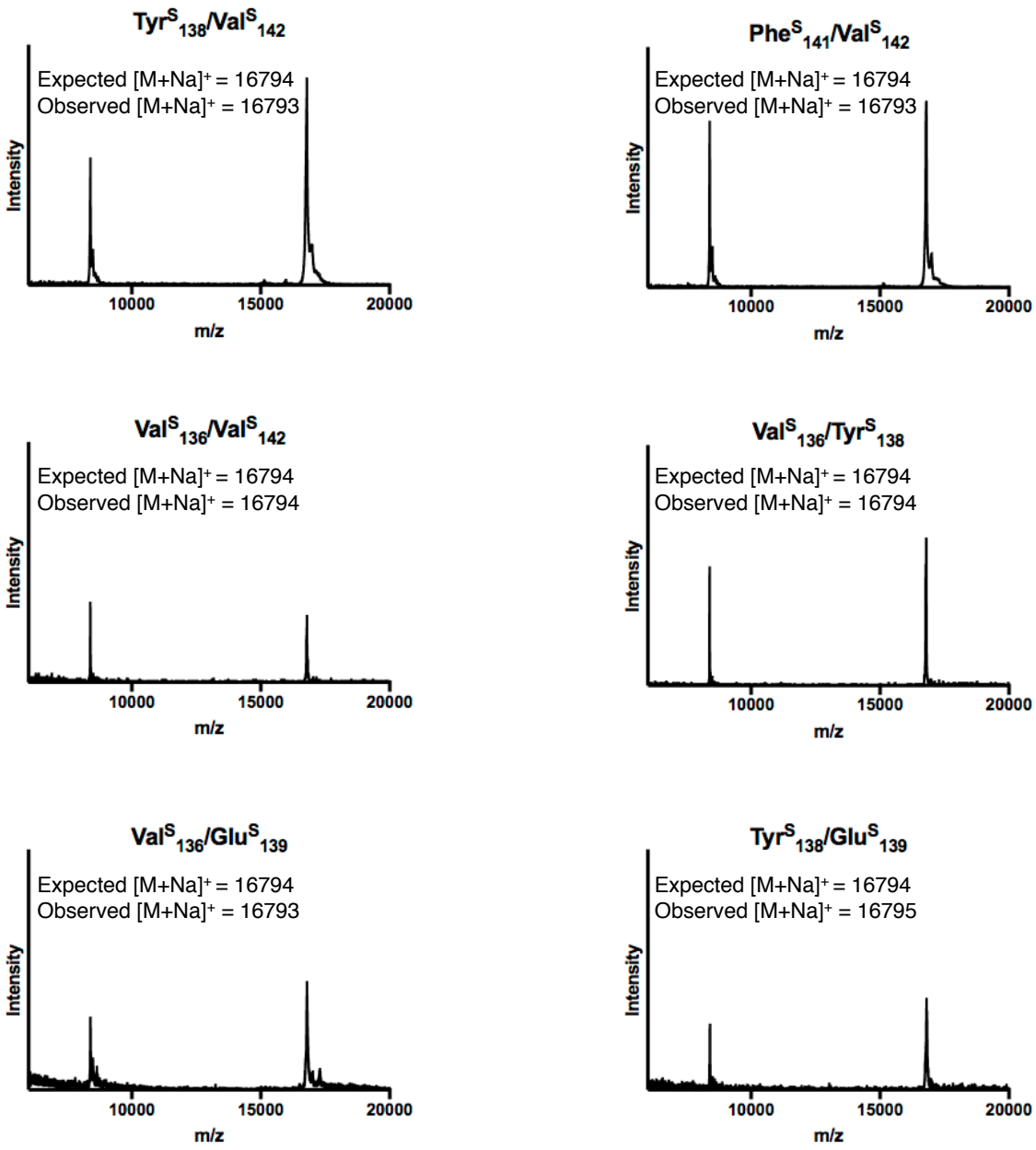

Figure S1: MALDI-MS traces showing pure CaM^{SS} proteins used for CD and fluorescence experiments.

Trypsin Digest of $Val^{S}_{136}/Tyr^{S}_{138}$ CaM

To ensure that the dithioamides are stable and unmodified during the entire purification and capping process, a trypsin digestion was performed on holo CaM-$Cys^{Q}_{135}Val^{S}_{136}/Tyr^{S}_{138}$. 200 µL of the CaM sample used for CD spectra acquisition (see below) was incubated with 10 µL of 0.5 µg/mL sequencing grade trypsin at 37 °C for 20 hours. The reaction was then analyzed by MALDI-MS and MALDI-TOF tandem MS/MS fragmentation. The parent mass and resulting fragmentation pattern are consistent with the presence of both intact thioamides and a singly alkylated Cys residue (see Figures **S2** and **S3** and Table **S5**).

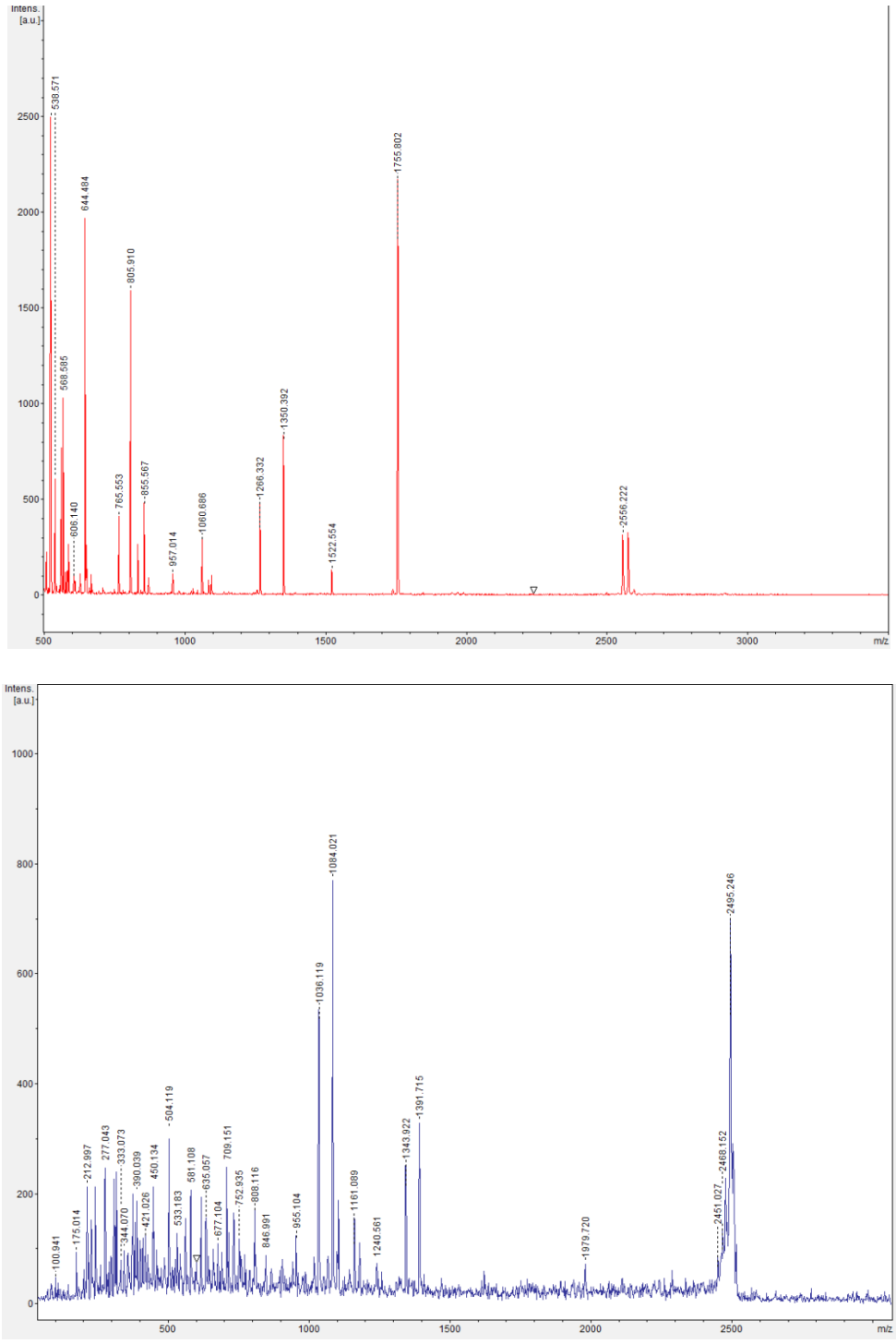

Figure S2: Top: Trypsin digest of CaM Val^{S}_{136}/Tyr^{S}_{138} showing the mass of the desired fragment containing the both thioamides and the alkylated Cys^{Q} (expected $[M+H]^{+}$ = 2555.89 Da, observed 2556.22 Da) Bottom: Tandem MS/MS fragmentation of the tryptic peptide corresponding to the sequence shown in Figure **S3**.

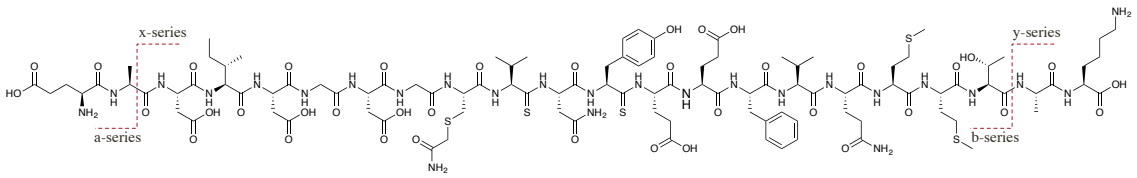

Figure S3: Fragmentation patterns of the H_2N-EADIDGDGC^{Q}V^{S}NY^{S}EEFVQMMTAK-OH tryptic peptide.

Table S5: Expected (black) and observed (red) MS/MS fragment m/z (a-, b-, x- and y- series ions) for the tryptic peptide H_2N-EADIDGDGC^{Q}V^{S}NY^{S}EEFVQMMTAK-OH. Nearly complete coverage of the peptide is observed.

Sequence	Observed Series	a (m/z)	Obs a (m/z)	b (m/z)	Obs b (m/z)	x (m/z)	Obs x (m/z)	y (m/z)	Obs y (m/z)
E	a,b	102.113	100.941	130.123	129.065	---	---	2555.821	---
A	a,b,x	173.192	175.014	201.202	201.041	2452.699	2451.027	2426.706	---
D	a,b	288.280	288.021	316.290	316.039	2381.621	---	2355.627	---
I	a,b	401.440	401.095	429.450	429.133	2266.532	---	2240.538	---
D	b	516.528	---	544.538	544.129	2153.373	---	2127.379	---
G	---	573.580	---	601.590	---	2038.284	---	2012.290	---
D	x	688.669	---	716.679	---	1981.232	1979.720	1955.238	---
G	---	745.721	---	773.731	---	1866.144	---	1840.149	---
C^{Q}	y	905.899	---	933.909	---	1809.092	---	1783.098	1785.731
V^{S}	y	1004.395	---	1049.057	---	1647.668	---	1622.959	1622.559
N	b	1135.151	---	1163.161	1162.947	1548.995	---	1507.771	---
Y^{S}	b,y	1297.483	---	1342.392	1343.922	1419.667	---	1393.667	1391.709
E	b	1443.497	---	1471.507	1471.392	1255.516	---	1214.436	---
E	y	1572.613	---	1600.623	---	1110.315	---	1085.321	1084.365
F	b,y	1719.789	---	1747.799	1750.213	982.199	---	956.206	955.283
V	y	1818.922	---	1846.932	---	835.023	---	809.029	808.179
Q	x,y	1947.053	---	1975.062	---	735.891	733.961	709.896	709.140
M	y	2078.245	---	2106.255	---	607.759	---	581.766	581.112
M	y	2209.438	---	2237.448	---	476.567	---	450.573	450.990
T	b,x,y	2310.543	---	2338.552	2351.527	345.475	344.070	319.381	319.117
A	x,y	2381.622	---	2409.632	---	244.269	243.032	218.275	218.041
K	a,x,y	2509.796	2509.475	2537.806	---	173.191	175.014	147.197	147.055

CD Sample Preparation, Sample Measurements, and Fitting Procedures

CD samples were prepared as in Walters *et al.*[2] and CD spectra were acquired on samples with a final concentration between 10 and 15 μM (as determined by BCA assay). Each holo spectrum and thermal melt was acquired as a single sample and apo spectra and thermal melt acquisition were performed in duplicate. Each sample (300 μL) was added to a 1 mm path length Helma Analytics 110-QS CD cuvette and loaded into a Jasco J-1500 CD Spectrometer. CD wavelength scans were taken at 25 °C by scanning at a 1 nm step between 350 nm and 190 nm with a bandwidth of 1 nm and an averaging time of 8 s per measurement. Background spectra were obtained by measuring the CD signal of the relevant buffer in each cuvette with an averaging time of 2 s. The raw signal (θ_d, mDeg) from each sample was background subtracted against the blanks and converted to molar residue ellipticity (θ_{MRE}) using

$$\theta_{MRE} = \theta_d/(cln_R) \quad \text{(S1)}$$

where *c* is the concentration (M), l is the path length (1 mm), and n_R is the number of residues in the protein.

Fitting was performed via a three-state fit method as previously described.[2] In this model, the protein undergoes two transitions: F→I and I→U, where F, I, and U are the folded, intermediate, and unfolded states, respectively. The equations used here are adopted from Shea *et al.*[3] The folded, intermediate, and unfolded baselines were fit to $\theta_f = m_f T + b_f$, $\theta_i = m_i T + b_i$, and $\theta_u = m_u T + b_u$, respectively. In this case, m_i was constrained to the average of m_f and m_u as previously described.[3] The full data set was then fit to

$$\theta_{fit} = (\theta_f)(F_f) + (\theta_i)(F_i) + (\theta_u)(F_u) \quad \text{(S2)}$$

$$F_u = \frac{K_1 K_2}{1+K_1+K_1 K_2} \qquad F_i = \frac{K_1}{1+K_1+K_1 K_2} \qquad F_f = 1 - F_i - F_u \tag{S3}$$

$$K_n = e^{-\Delta G_n / RT} \tag{S4}$$

$$\Delta G_n(T) = \Delta H_n \left(1 - \frac{T}{T_{M_n}}\right) + \Delta C_{p_n} \left[\left(T - T_{M_n}\right) - (T)\left(Ln\left(\frac{T}{T_{M_n}}\right)\right)\right] \tag{S5}$$

where K_1 and K_2 are the equilibrium constants for the transitions F→I and I→U, respectively. F_f, F_i, and F_u are the calculated fractions of the total population that the folded, intermediate, and unfolded states make up at any given temperature. The heat capacity ΔC_{p_n} for each transition is set to zero in accordance with previous analyses of CaM unfolding.[3] ΔH_n and T_{M_n} are adjustable parameters for each transition. The RMSD between the observed θ_{MRE} and θ_{fit} was minimized against these adjustable parameters. A weighted fraction folded value $F_f^* = F_f + nF_i$ was generated to account for the contributions of both C- and N-terminal unfolding to the overall unfolding transition. Here, n is a weighting factor held constant to $n = 0.5$ to reflect the weighted contribution of m_i in θ_{fit}. A weighted average melting temperature of the two transitions (T_M*) is generated by finding T such that $\Delta G_1(T) + \Delta G_2(T) = 0$. T_M* corresponds to the midpoint of the F_f^* unfolding curve. ΔG_U for the total transition of F→U was calculated as a sum of ΔG_1(298.15) and ΔG_2(298.15). Initial guesses for ΔH_1, ΔH_2, T_{M1}, and T_{M2} were taken from single thioamide thermal melts (values obtained in Walters *et al.*[2]) as starting values. Representative traces of the raw data and fits, as well as the fractional population analysis, can be seen in Figures **S4-S8**. The fitted parameters are summarized in Table **S6**.

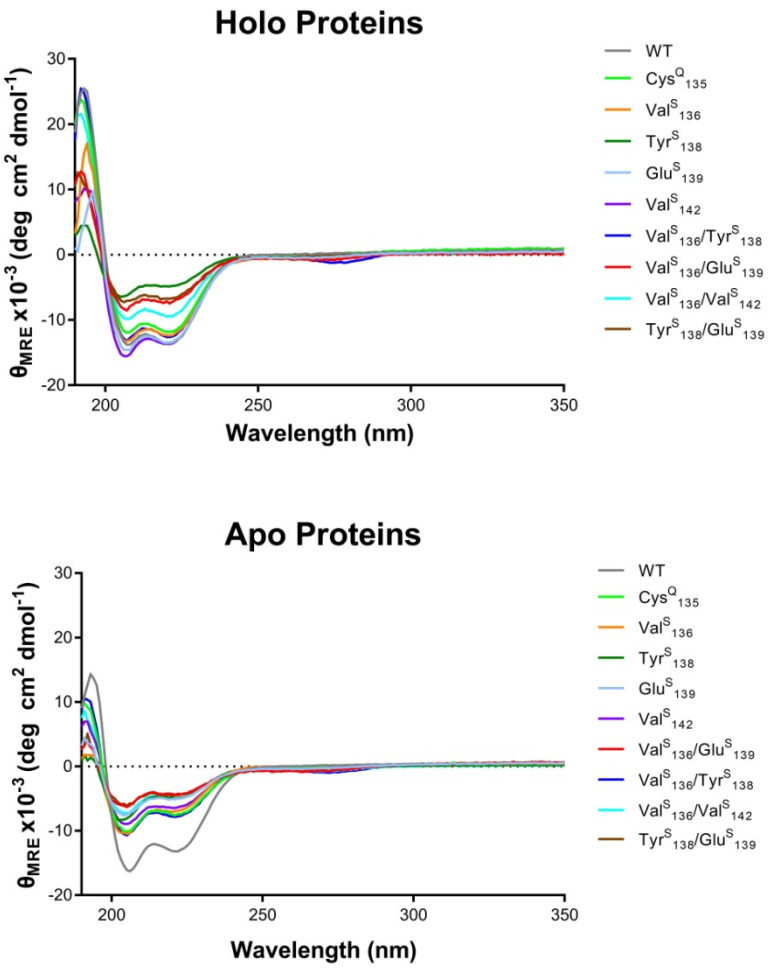

Figure S4: CD wavelength scans for dithioproteins each containing at least one predictively stabilizing mutation. Single thioamide protein wavelength scans are also shown for direct comparison. A significantly increased $\pi \rightarrow \pi^*$ single (centered at 270 nm) is observed in the $Val^{S}_{136}/Tyr^{S}_{138}$ protein (blue).

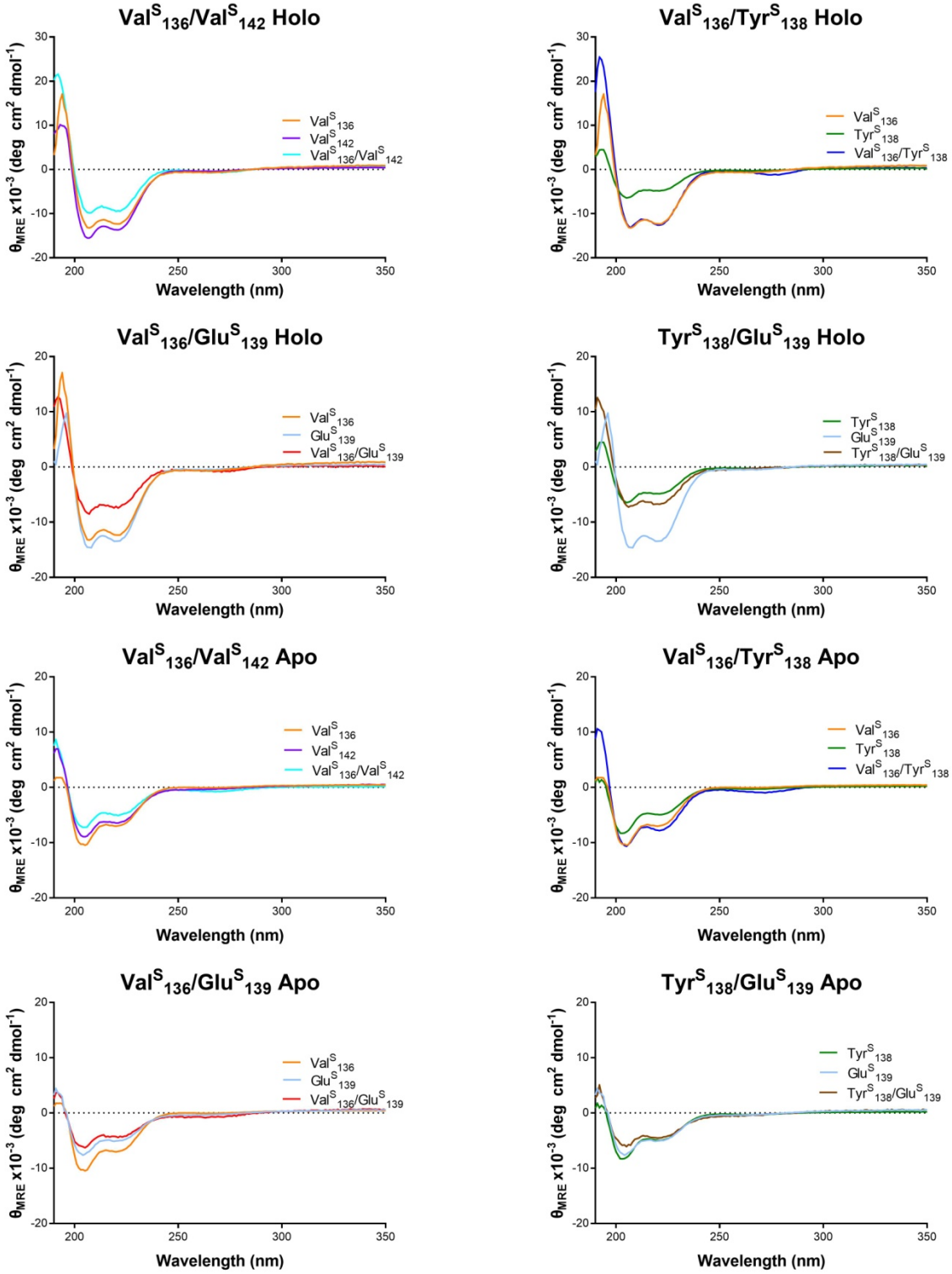

Figure S5: CD wavelength scans of each CaM^{SS} protein (holo and apo) plotted with their respective single thioamide scans from previous work.[2] Increased absorbance at 270 nm (thioamide CD signature) is observed for both Val$^S_{136}$/Val$^S_{142}$ and Val$^S_{136}$/Tyr$^S_{138}$ proteins.

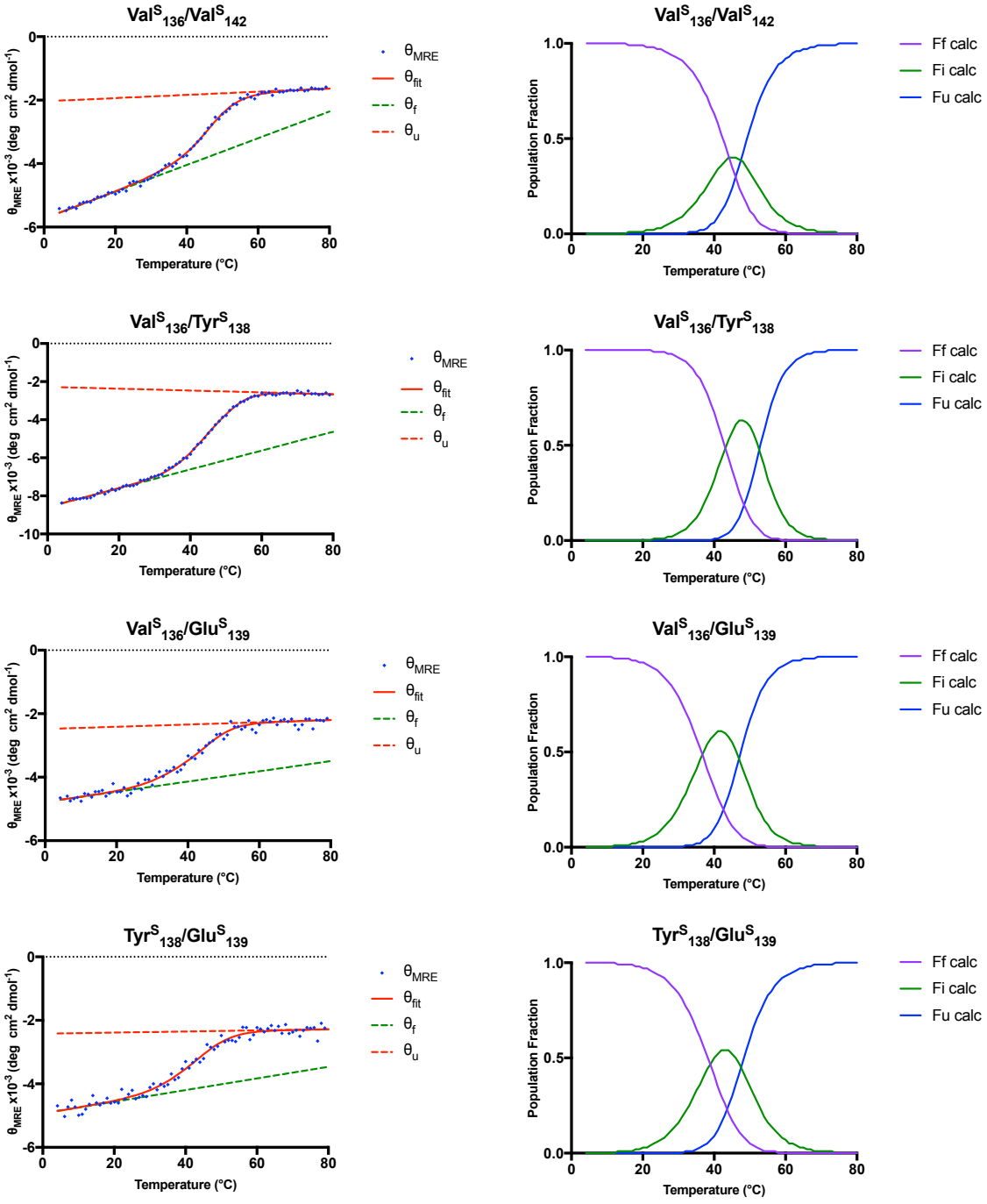

Figure S6: Plots generated using the three state fitting method for all CaM^{SS} variants. Left: For each CaM^{SS} variant, a representative set of raw data (θ_{MRE}) and fits generated from θ_{fit}, θ_f, and θ_u. Right: The averaged fraction folded (F_f, purple), fraction intermediate (F_i, green), and fraction unfolded (F_u, blue) plots from the three replicates.

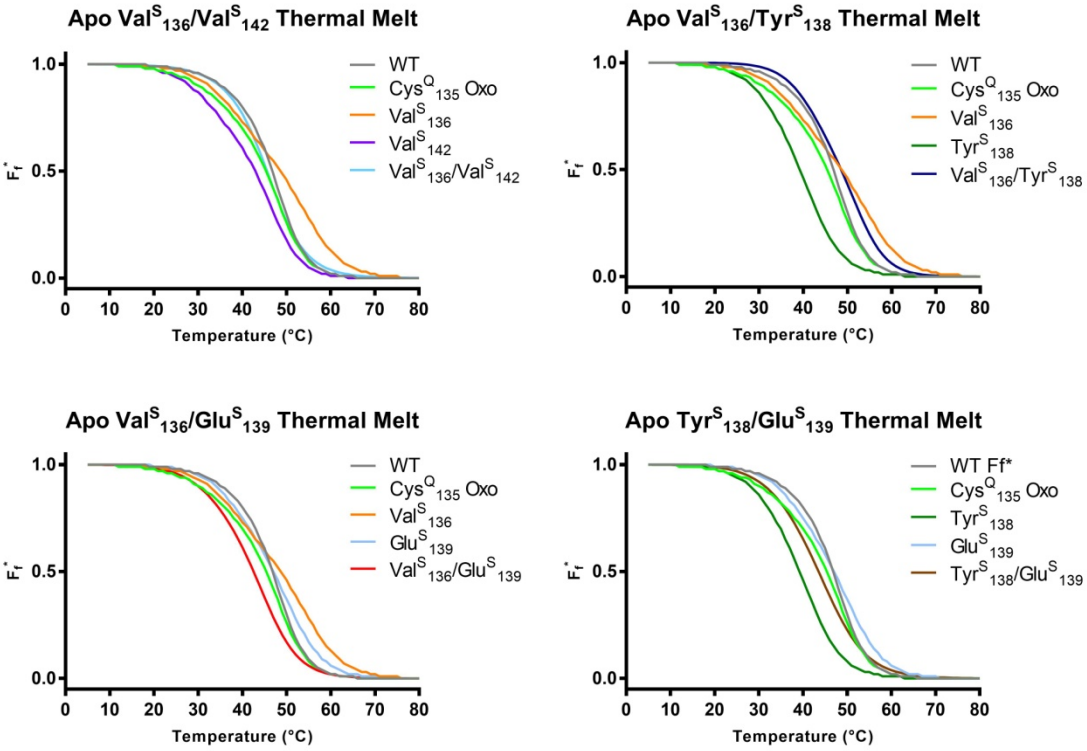

Figure S7: Individual fraction folded (F_f*) plots for CaM^{SS} thermal melts showing corresponding single thioamide thermal melts and the Cys^{Q} oxo and wild type controls.

Table S6: Thermodynamic values for CaM^{SS} variants compared to their single thioamide congeners.

CaM Variant	T_{M1}[a] (°C)	ΔH_1 (kcal mol^{-1})	T_{M2} (°C)	ΔH_2[b] (kcal mol^{-1})	T_M*[c] (°C)	ΔT_m* (°C)	ΔG_U[d] (kcal mol^{-1})	$\Delta\Delta G_U$ (kcal mol^{-1})
WT	43.5 ± 0.6	33.1 ± 0.8	48.6 ± 0.6	60.5 ± 0.7	46.8 ± 0.3	---	6.4 ± 0.2	---
Cys$^{Q}_{135}$ Oxo	38.9 ± 0.8	30.2 ± 0.9	48.8 ± 0.7	61.7 ± 0.8	45.5 ± 0.4	---	5.9 ± 0.1	---
Val$^{S}_{136}$	39.6 ± 0.5	36.7 ± 0.6	55.3 ± 0.8	52.0 ± 0.5	48.6 ± 0.7	3.1	6.5 ± 0.1	0.6
Tyr$^{S}_{138}$	34.7 ± 0.8	39.7 ± 0.7	43.0 ± 0.9	51.1 ± 1.0	39.3 ± 0.8	-6.2	4.1 ± 0.2	-1.8
Glu$^{S}_{139}$	40.7 ± 0.7	40.1 ± 0.4	51.9 ± 0.6	53.9 ± 0.9	47.0 ± 0.1	1.6	6.4 ± 0.1	0.5
Val$^{S}_{142}$	36.4 ± 0.6	35.5 ± 0.8	48.4 ± 0.8	62.9 ± 0.9	44.0 ± 0.7	-1.5	5.8 ± 0.2	-0.1
Val$^{S}_{136}$/Tyr$^{S}_{138}$	43.0 ± 0.1	48.0 ± 1.7	53.0 ± 0.6	62.1 ± 1.6	48.6 ± 0.2	3.1	8.1 ± 0.3	2.2
Val$^{S}_{136}$/Glu$^{S}_{139}$	37.4 ± 1.0	36.0 ± 1.5	46.4 ± 0.8	50.5 ± 2.7	42.6 ± 0.1	-2.9	4.8 ± 0.2	-1.1
Val$^{S}_{136}$/Val$^{S}_{142}$	43.8 ± 0.5	32.9 ± 0.7	47.0 ± 0.7	42.9 ± 0.2	45.6 ± 0.6	0.1	4.9 ± 0.1	-1.0
Tyr$^{S}_{138}$/Glu$^{S}_{139}$	38.8 ± 0.0	36.3 ± 1.9	47.6 ± 0.1	43.4 ± 2.0	43.6 ± 0.2	-2.2	4.6 ± 0.1	-1.3

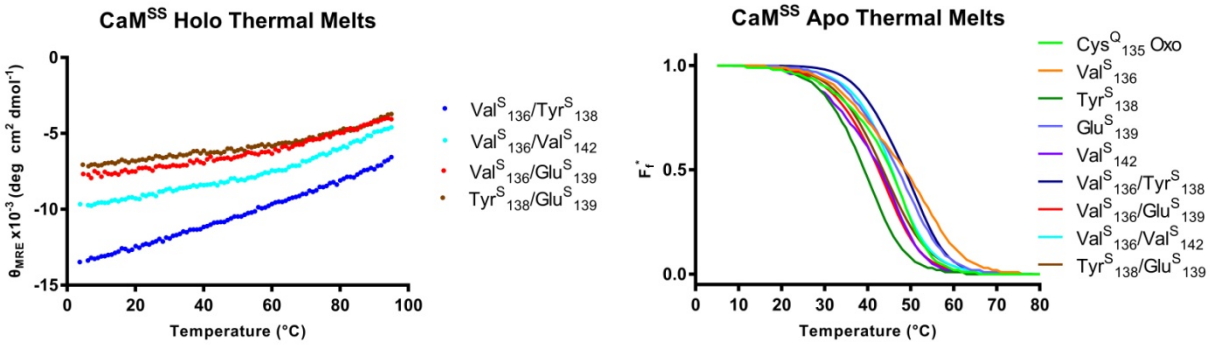

Figure S8: Left: Holo dithioCaM MRE values plotted as a function of temperature. All dithioproteins have T_M values greater than 80 °C, in agreement with oxo and single thioamide controls. Right: Transformed apo thermal melts plotted as fraction folded (F_f*) fits that include a weighted contribution from the intermediate. Melting curves were obtained by measuring the θ_{222} at 1 °C increments in 10 mM Tris, pH 7.5 with either 0.5 mM EDTA (apo) or 2 mM $CaCl_2$ (holo).

Structural Anaylsis of Thioamide Effects

Our analysis of thioamide thermostability effects in CaM focuses on structures of the apo protein from *Rattus norvegicus* (crystal, PDB entry 1QX5) and *Xenopus laevis* (NMR, PDB entry 1CFD).[4, 5] It should be noted that crystal packing in the 1QX5 structure gives rise to non-native intermolecular interactions, but these are analogous to intramolecular interactions observed in the NMR structure (see Fig. **S9**). Distance parameters for the thioamide substitutions studied here are reported in Table **S7**. The register of the C-terminal helix is slightly different in 1QX5 and 1CFD, due to an alteration of the hydrogen bonding partner for the Asn_{137} sidechain. The 1CFD helical register leads to a very short hydrogen bonding distance for the carbonyl of Tyr_{138}, which is disrupted by thioamide substitution. We hypothesize that thioamide substitution at Val_{136} and Tyr_{138} leads to a 1QX5-like conformation wherein strong N-H hydrogen bond donation from Val^S_{136} and Tyr^S_{138} can simultaneously stabilize respective interactions with the sidechains of Glu_{140} and Asn_{137} (Figs. **S10**-**S11**). The 1QX5-like conformation would more readily accommodate the Tyr^S_{138} thiocarbonyl.

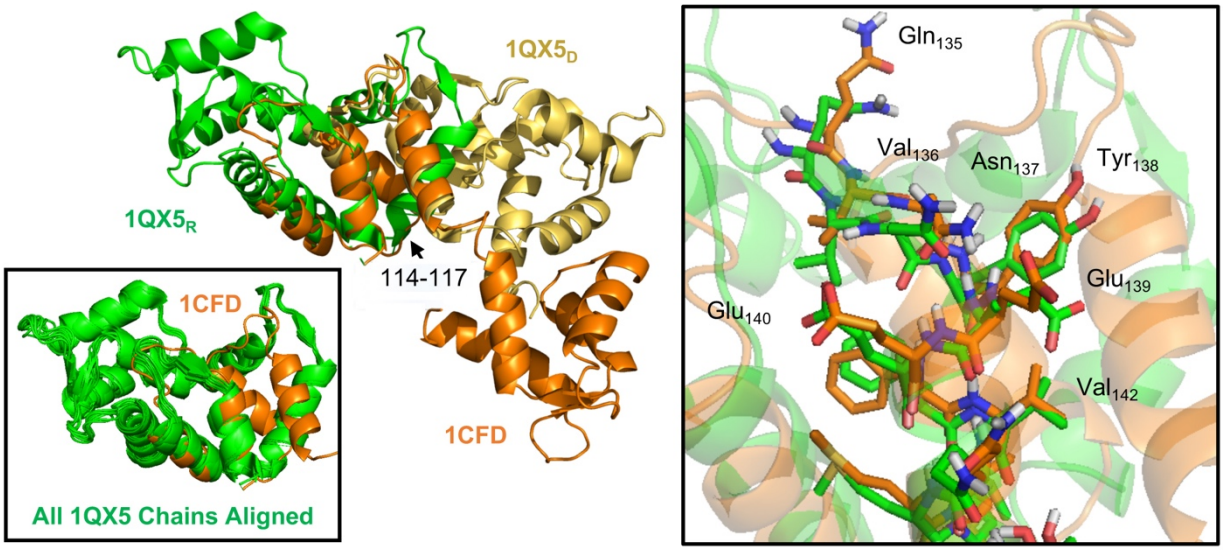

***Figure S9*:** Apo CaM structures. Overlay of C-terminal helix of 1CFD NMR structure with corresponding helix in chain$_R$ of 1QX5 crystal structure showing alignment of residues 118-148. Twisting about the 114-117 segment prevents simultaneous alignment of the rest of the CaM sequence. Residues 81-101 in chain$_D$ of 1QX5 structure make intermolecular contacts similar to the intramolecular contacts of residues 81-101 in 1CFD. Left Inset: All eight chains in 1QX5 structure aligned, showing identical folds. Right Inset: C-terminal helices of 1CFD and 1QX5 structures.

***Table S7**:* Distances and angles for hydrogen bonds at sites of thioamide substitution in apo CaM structures from PDB entries 1CFD and 1QX5. 1QX5 distances are averages of distances in all 8 chains. X denotes site of thioamide insertion. Hydrogen bonding partners can be seen in Figs. **S10**-**S11**.

	C=X--N Dist. (Å)		C=X--N Angle (º)		N^X--O=C Dist. (Å)		N^X--O=C Angle (º)	
Residue	1CFD	1QX5	1CFD	1QX5	1CFD	1QX5	1CFD	1QX5
Val^S_{136}	3.4	3.1	137	151	---	---	---	---
Tyr^S_{138}	2.6	3.1	165	157	---	2.8*	---	123*
Glu^S_{139}	3.4	3.0	145	144	3.3*	---	130*	---
Val^S_{142}	3.3	3.3	160	152	3.4	3.0	150	147

*Asn_{137} sidechain forms hydrogen bonds with either Tyr_{138} or Glu_{139}.

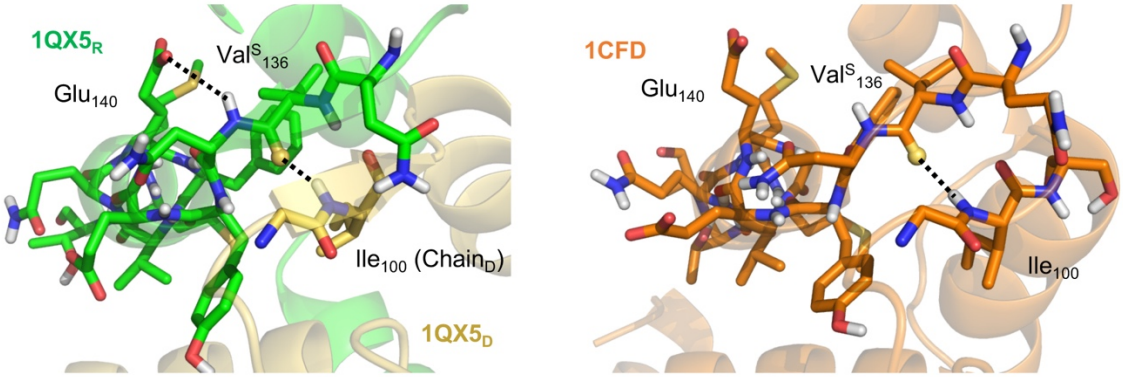

Figure S10: Hydrogen bonding of Val^{S}_{136}. In the 1QX5 structure, Val_{136} donates a hydrogen bond to the sidechain of Glu_{140}.

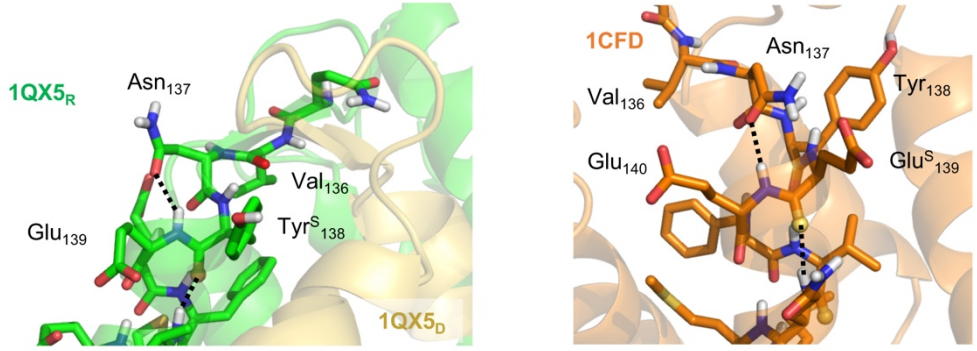

Figure S11: Hydrogen bonding of Tyr^{S}_{138} and Glu^{S}_{139}. 1QX5 structure shows the potential stabilizing hydrogen bond from the N-H of the Tyr^{S}_{138} thioamide to the sidechain carbonyl of Asn_{137}. 1CFD structure shows the potential stabilizing hydrogen bond from the N-H of the Glu^{S}_{139} thioamide to the sidechain carbonyl of Asn_{137}.

Peptide Binding Assays

All protein and peptides were dissolved in 15 mM HEPES, 140 mM KCl, 6 mM $CaCl_2$ pH 6.70 and centrifuged at 13,200 rpm on a tabletop centrifuge for 10 min at 4 °C to remove any insoluble aggregates. Concentrations of each of the CaM mutants were determined using the FluoroProfile® Protein Quantification Kit by Sigma Aldrich, using a series of WT CaM dilutions as a standard. W-pOCNC concentration was determine by absorbance spectroscopy based on the previously published extinction coefficient (ε_{278}=5700 $M^{-1}cm^{-1}$).[6] The W-pOCNC concentration was 1 μM in each sample, with CaM protein concentrations of either 0.5 or 2 μM. Samples were prepared and briefly vortexed prior to measurements. Spectra were acquired via excitation at 295 nm and emission collection over 305-450 nm with all slit widths set to 5 nm with an integration time of 0.25 seconds for each 1 nm step. Measurements were taken in triplicate.

Fitting Fluorescence Data

Fluorescence emission spectra were fit using the same method as previously described[4] to determine both the concentration of free W-pOCNC peptide and the relative quenching of the bound population by mono/dithioamide containing protein. Each emission spectrum was fit to a linear sum of the free and bound W-pOCNC spectrum by determining the least square difference detailed in Eq. S6 below:

$$\sum_{\lambda}\left(I(\lambda)_{Assay} - AI(\lambda)_{Free} - BI(\lambda)_{Bound} - CI(\lambda)_{Scatter} - DI(\lambda)_{Background}\right)^2 \rightarrow \min \qquad \text{(S6)}$$

In the above equation $I(\lambda)_{Assay}$ represents the measured emission spectrum of the sampling containing both W-pOCNC and the modified CaM protein. This emission is a combination of the emission profiles of free and bound W-pOCNC represented as $I(\lambda)_{Free}$ and $I(\lambda)_{Bound}$ and. The $I(\lambda)_{Free}$ spectrum was determined from 1 μM W-pOCNC in buffer while the $(\lambda)_{Bound}$ spectrum was collected on a 4:1 sample of WT CaM:W-pOCNC using the previously described settings. The difference between the sum of these spectra and the measured sample emission was minimized by adjusting the linear weights of the free and bound spectra represented as *A* and *B* respectively. The final two terms represent the minor scatter which likely originated from incomplete removal of all small aggregated species that were not fully solubilized following lyophilization, $I(\lambda)_{Scatter}$, and a small amount of background in each spectrum originating from intrinsic fluorescence of the mutant CaM samples, $I(\lambda)_{Background}$. The spectral profiles were obtained from 4 μM WT CaM and 2 μM Val^{S}_{136} CaM respectively and the linear contributions of these spectra are represented as *C* and *D*. Table **S7** contains all of the resultant values from the fitting.

Determining Percent Bound and Quenching Efficiency

Following fitting of the emission spectra, the percent bound and the quenching efficiency were determined from the *A* and *B* coefficients along with Eq S7 and S8 below.

$$F_B = 1 - F_A = 1 - A \qquad \text{(S7)}$$

$$Q_E = \frac{B}{F_A} \qquad \text{(S8)}$$

The fraction of bound W-pOCNC, F_B, can be directly computed from the fraction of free W-pOCNC, F_A, which is directly equivalent to *A*. The fraction bound can subsequently be converted to percent bound. The quenching efficiency, Q_E, is then determined as the fraction of observed fluorescence from bound W-pOCNC, *B*, divided by the fraction bound determined from the reduction of free W-pOCNC signal. The resultant values are listed in Table **S7**.

Table S7: Resulting fit parameters, percent bound and quenching efficiency values.

	CaM: W-pOCNC	A	B	C	D	% Bound	Error	Q_E	Error
WT	0.5:1	0.732	0.249	0.147	0.009	26.816	0.436	0.070	0.008
	2:1	0.011	0.966	0.542	0.061	98.852	0.380	0.022	0.004
	Avg							0.046	0.004
Cys^{Q}_{135}	0.5:1	0.421	0.400	0.225	0.060	57.935	0.313	0.309	0.009
	2:1	0.000	0.938	0.025	0.004	100.000	0.359	0.062	0.004
	Avg							0.185	0.005
Val^{S}_{136}	0.5:1	0.790	0.071	0.007	0.252	21.021	0.574	0.660	0.010
	2:1	0.419	0.149	0.179	0.997	58.124	0.713	0.744	0.021
	Avg							0.702	0.012
Tyr^{S}_{138}	0.5:1	0.746	0.087	0.351	0.267	25.356	0.558	0.656	0.010
	2:1	0.506	0.202	1.103	0.892	49.383	0.733	0.591	0.018
	Avg							0.623	0.010
Glu^{S}_{139}	0.5:1	0.647	0.180	0.360	0.252	35.271	0.499	0.488	0.010
	2:1	0.311	0.372	1.001	0.689	68.872	0.542	0.460	0.019
	Avg							0.474	0.011
Val^{S}_{142}	0.5:1	0.751	0.092	0.509	0.415	24.870	0.634	0.630	0.012
	2:1	0.180	0.222	1.574	1.332	81.990	0.777	0.730	0.048
	Avg							0.680	0.024
Val^{S}_{136}/ Tyr^{S}_{138}	0.5:1	0.847	0.059	0.125	0.076	15.293	0.524	0.614	0.009
	2:1	0.371	0.184	0.422	0.288	62.868	0.363	0.707	0.012
	Avg							0.660	0.007
Val^{S}_{136}/ Glu^{S}_{139}	0.5:1	0.909	0.000	0.713	0.626	9.076	1.382	1.000	0.022
	2:1	0.401	0.000	2.502	2.164	59.933	1.519	1.000	0.054
	Avg							1.000	0.029
Val^{S}_{136}/ Val^{S}_{142}	0.5:1	0.695	0.000	0.461	0.443	30.464	0.616	1.000	0.013
	2:1	0.000	0.000	1.694	1.566	100.000	0.797	1.000	0.000
	Avg							1.000	0.006
Tyr^{S}_{138}/ Glu^{S}_{139}	0.5:1	0.879	0.017	0.487	0.511	12.137	1.201	0.861	0.019
	2:1	0.549	0.043	1.358	1.366	45.071	1.174	0.904	0.029
	Avg							0.883	0.018

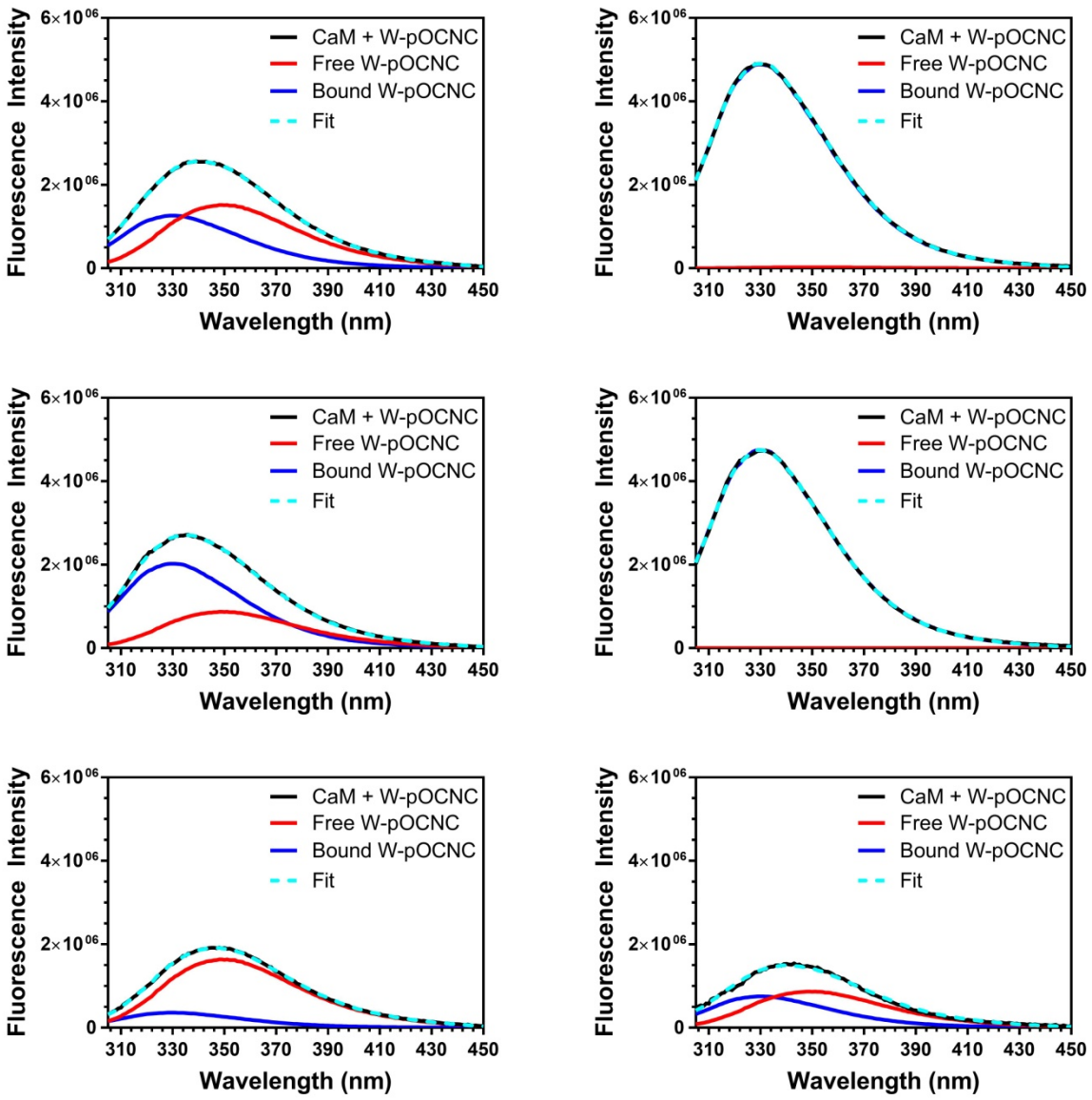

Figure S12: Fluorescence spectra of the W-pOCNC peptide bound to WT (Top), Cys^{Q}_{135} Oxo (Middle), and Val^{S}_{136} (Bottom) CaM in samples with ratios of 0.5:1 (Left) and 2:1 (Right) CaM to W-pOCNC. CaM + W-pOCNC shows $I(\lambda)_{Assay}$ - $CI(\lambda)_{Scatter}$ - $DI(\lambda)_{Background}$, while Free and Bound W-pOCNC show $AI(\lambda)_{Free}$ and $BI(\lambda)_{Bound}$ respectively, and Fit is $AI(\lambda)_{Free}$ + $BI(\lambda)_{Bound}$.

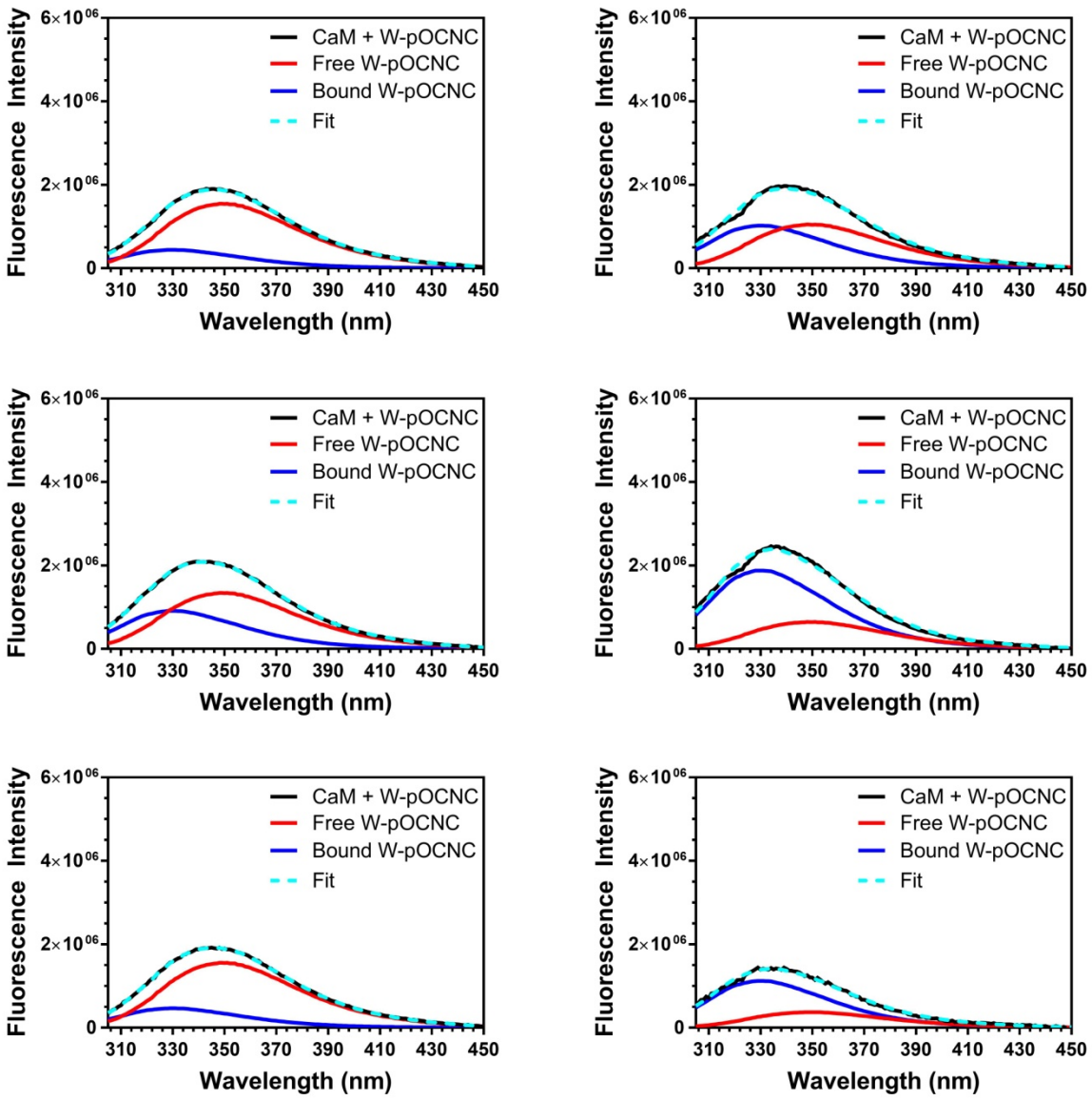

Figure S13: Fluorescence spectra of the W-pOCNC peptide bound to Tyr^{S}_{138} (Top), Glu^{S}_{139} Oxo (Middle), and Val^{S}_{142} (Bottom) CaM in samples with ratios of 0.5:1 (Left) and 2:1 (Right) CaM to W-pOCNC. CaM + W-pOCNC shows $I(\lambda)_{Assay}$ - $CI(\lambda)_{Scatter}$ - $DI(\lambda)_{Background}$, while Free and Bound W-pOCNC show $AI(\lambda)_{Free}$ and $BI(\lambda)_{Bound}$ respectively, and Fit is $AI(\lambda)_{Free}$ + $BI(\lambda)_{Bound}$.

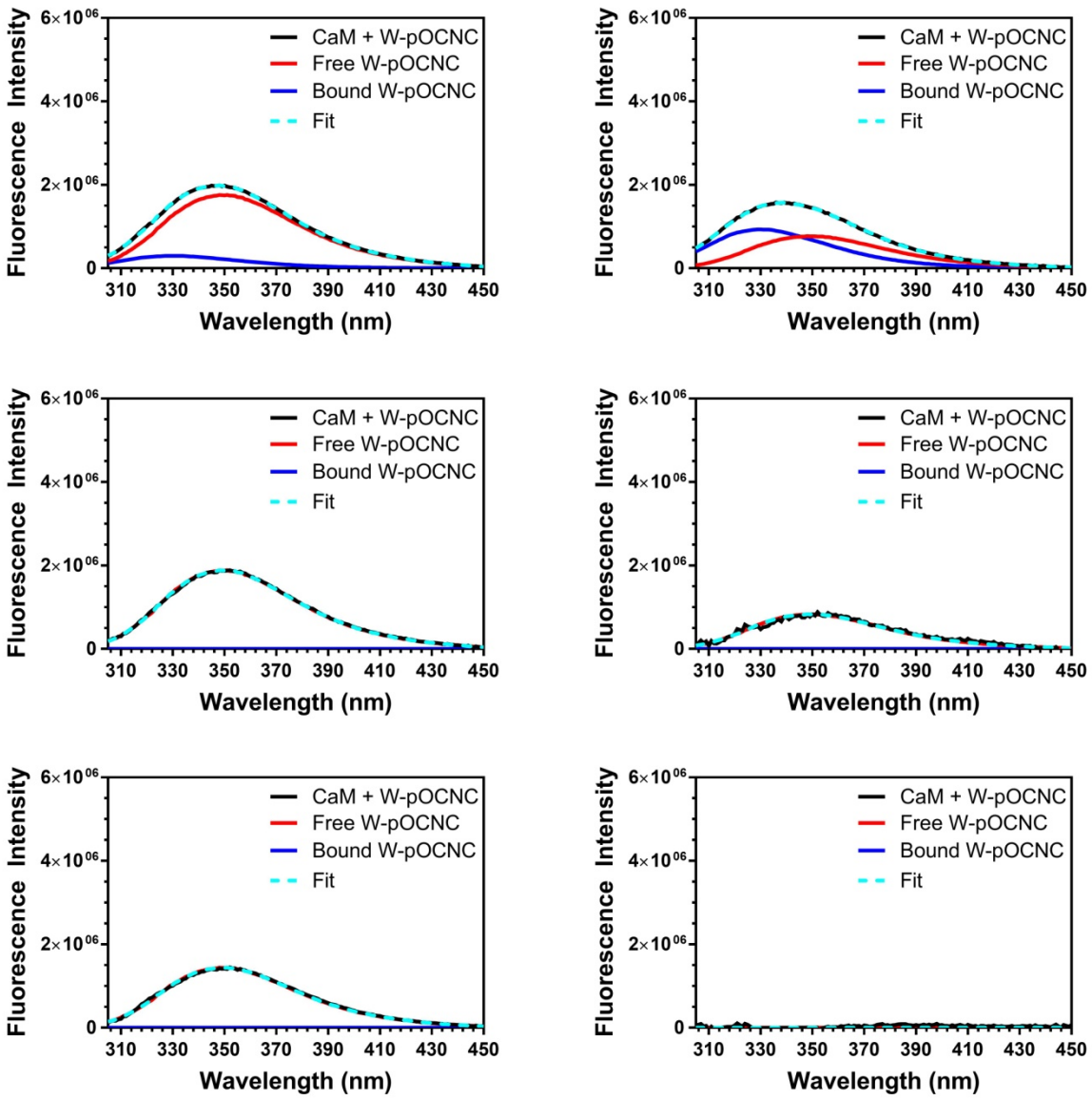

Figure S14: Fluorescence spectra of the W-pOCNC peptide bound to $Val^{S}_{136}/Tyr^{S}_{138}$ (Top), $Val^{S}_{136}/Glu^{S}_{139}$ (Middle), and $Val^{S}_{136}/Val^{S}_{142}$ (Bottom) CaM in samples with ratios of 0.5:1 (Left) and 2:1 (Right) CaM to W-pOCNC. CaM + W-pOCNC shows $I(\lambda)_{Assay}$ - $CI(\lambda)_{Scatter}$ - $DI(\lambda)_{Background}$, while Free and Bound W-pOCNC show $AI(\lambda)_{Free}$ and $BI(\lambda)_{Bound}$ respectively, and Fit is $AI(\lambda)_{Free}$ + $BI(\lambda)_{Bound}$.

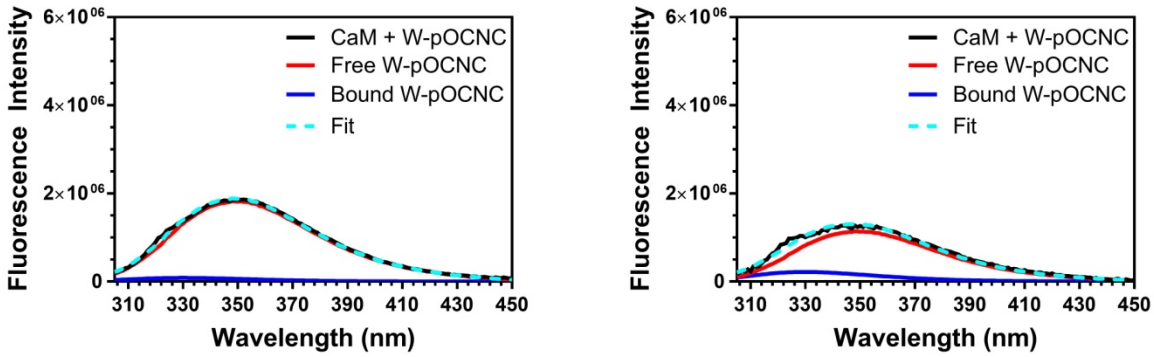

Figure S15: Fluorescence spectra of the W-pOCNC peptide bound to Tyr^{S}_{138}/Glu^{S}_{139} CaM in samples with ratios of 0.5:1 (Left) and 2:1 (Right) CaM to W-pOCNC. CaM + W-pOCNC shows $I(\lambda)_{Assay}$ - $CI(\lambda)_{Scatter}$ - $DI(\lambda)_{Background}$, while Free and Bound W-pOCNC show $AI(\lambda)_{Free}$ and $BI(\lambda)_{Bound}$ respectively, and Fit is $AI(\lambda)_{Free}$ + $BI(\lambda)_{Bound}$.

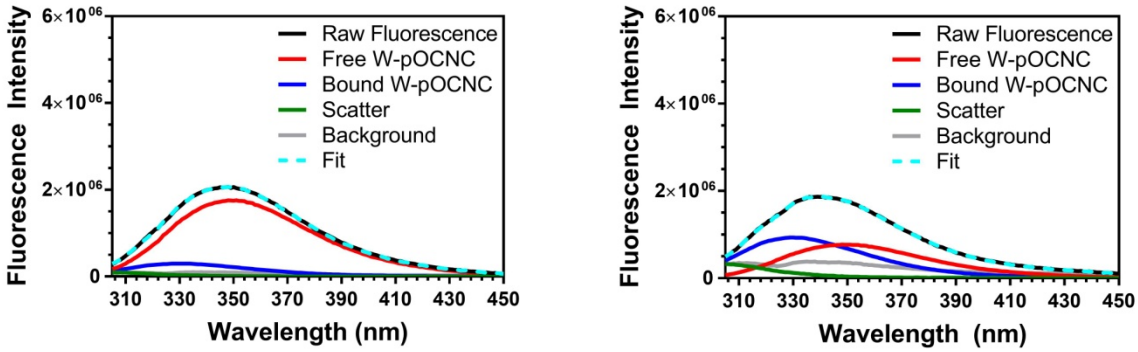

Figure S16: Example of contribution of all fitting components to overall spectral profile. Fluorescence spectra of the W-pOCNC peptide bound to Val^{S}_{136}/Tyr^{S}_{138} CaM in samples with ratios of 0.5:1 (Left) and 2:1 (Right) CaM to W-pOCNC. Raw Fluorescence shows $I(\lambda)_{Assay}$, while Free and Bound W-pOCNC along with Scatter and Background show the linearly weighted spectra of each component. Fit shows the sum of all linearly weighted components.

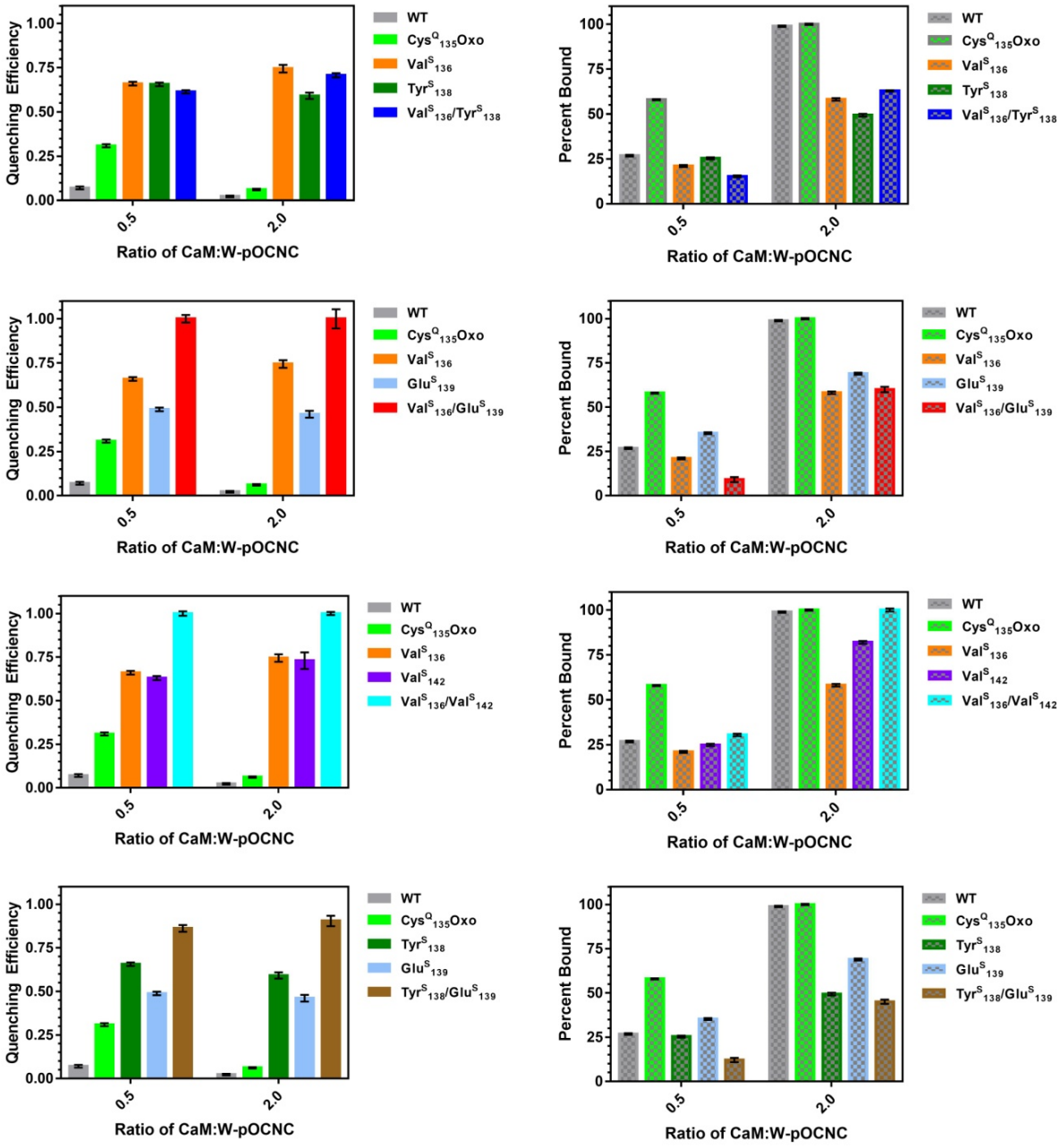

Figure S17: Individual plots of CaM- W-pOCNC binding experiments for Val$^{S}_{136}$/Tyr$^{S}_{138}$ (Top), Val$^{S}_{136}$/Glu$^{S}_{139}$ (Upper Middle), Val$^{S}_{136}$/Val$^{S}_{142}$ (Lower Middle), and Tyr$^{S}_{138}$/Glu$^{S}_{139}$ (Bottom) along with the related monothioamide CaM proteins showing the quenching efficiencies (left) and percent of W-pOCNC bound (right) at varying stoichiometric ratios of CaM: W-pOCNC.

Distances Between W-pOCNC Trp and Thioamide

Distances were extracted from NMR structural models (PDB 1SY9) of CaM bound to pOCNC for comparison to the quenching efficiency of each thioamide substitution. The average distances from the twenty structural models were computed for each position using Biopython and are reported in Table **S8**. Distances were measured between the amide carbon of the thioamide containing residue and the beta-carbon of the third residue of the bound peptide which is Phe.

Table S8: Average distances from PDB 1SY9 compared to quenching efficiencies from single thioamide introduction.

Thioamide Position	Avg. Distance (Å)	Q_E
Val 136	11.2 ± 0.5	0.70 ± 0.01
Tyr 138	13.4 ± 0.5	0.62 ± 0.01
Gly 139	13.1 ± 0.5	0.47 ± 0.01
Val 142	11.3 ± 0.4	0.68 ± 0.02

References

1. M. A. Shalaby, C. W. Grote and H. Rapoport, *J. Org. Chem.*, 1996, **61**, 9045-9048.
2. C. R. Walters, D. M. Szantai-Kis, Y. Zhang, Z. E. Reinert, W. S. Horne, D. M. Chenoweth and E. J. Petersson, *Chem. Sci.*, 2017, **8**, 2868-2877.
3. B. R. Sorensen and M. A. Shea, *Biochemistry*, 1998, **37**, 4244-4253.
4. M. A. Schumacher, M. Crum and M. C. Miller, *Structure*, 2004, **12**, 849-860.
5. H. Kuboniwa, N. Tjandra, S. Grzesiek, H. Ren, C. B. Klee and A. Bax, *Nat. Struct. Mol. Biol.*, 1995, **2**, 768-776.
6. J. M. Glasscock, Y. Zhu, P. Chowdhury, J. Tang and F. Gai, *Biochemistry*, 2008, **47**, 11070-11076.